

# Catalytic Activity of Synthesized NiMo Catalysts on Walnut Shell Activated Carbon for Heavy Naphtha Hydrotreating

Foroozandeh, Amin; Hatefirad, Parvaneh; Safaei Mahmoudabadi, Zohal;  
Tavasoli, Ahmad\*<sup>+</sup>

School of Chemistry, College of Science, University of Tehran, Tehran, I.R. IRAN

**ABSTRACT:** Hydrotreating of heavy naphtha using highly active NiMo catalysts on walnut shell activated carbon (NiMo-WAC) nanocatalysts is a new technology for clean fuel production. In this research, pyrolysis of the walnut shell as a scalable, low-cost, and high-yield method was used to synthesize chemically activated carbon in the presence of  $ZnCl_2$ , as activating agent. To enhance the catalytic conversion, walnut shell active carbon was functionalized with HCL,  $HNO_3$ , and  $H_2SO_4$  to prepare NiMo-WAC1, NiMo-WAC2, and NiMo-WAC3 respectively. These nanocatalysts were synthesized through the incipient wetness impregnation method and characterized by X-Ray Diffraction (XRD), Fourier Transform InfraRed (FT-IR) spectroscopy, Inductively Coupled Plasma-atomic emission (ICP) spectroscopy, Field Emission Scanning Electron Microscopy (FESEM), Brunauer–Emmett–Teller (BET) surface area, Temperature-Programmed Desorption (TPD) and Temperature-Programmed Reduction (TPR) techniques. CHNS (Eager 300 for EA1112) was used to study elemental analysis of the walnut shell feedstock used for active carbon synthesis. Different operating parameters including temperature, pressure, LHSV, and  $H_2$ /feed (heavy naphtha) ratio for hydrodesulfurization (HDS) reactions were explored by evaluating NiMo-WAC nanocatalysts catalytic activity. HDS of heavy naphtha with 2491 ppm of sulfur in the operation condition of temperature: 290 °C, pressure: 30 bar,  $H_2$ /oil: 100 NL/L, and LHSV: 3.3  $h^{-1}$  showed considerably higher activity of NiMo-WAC2 nanocatalyst, less than 10 ppm in the product, than NiMo- $\gamma$ - $Al_2O_3$  as a commercial and reference catalyst, maximum 104 ppm in the product, and this is economically valuable.

**KEYWORDS:** Hydrotreating; Walnut shell activated carbon; Nanocatalyst, Heavy naphtha; HDS; NiMo catalysts.

## INTRODUCTION

Due to the industrialization of countries, the release of various categories of hazardous compounds, into the environment has become a serious concern. Sulfur and nitrogen content of hydrocarbon fuels can cause

environmental problems, regarding air pollution [1–3]. Nowadays, the increase of greenhouse gases concentrations in the atmosphere including nitrous oxide, carbon dioxide, etc. during industrial activities and combustion of fossil

\* To whom correspondence should be addressed.

+ E-mail: [tavasoli.a@ut.ac.ir](mailto:tavasoli.a@ut.ac.ir)

1021-9986/2023/1/38-50

13/\$/6.03

fuels is one of the most significant worldwide challenges[4–6]. Besides, high corrosive impact and also effect of sulfur on deactivation of catalysts in catalytic reactions in industries such as petro-refineries has always attracted researchers' attention[7–9]. Catalytic hydrotreating technology in petro-refineries is fully developed to treat sulfur-rich fossil fuels in Hydro-DeSulfurization (HDS) process[10,11]. The objection materials mainly including, but are not solely limited to, sulfur, nitrogen, olefins and aromatics are removed from hydrocarbon fuels through selective reactions in presence of catalysts at a moderate to high pressure and temperature [12,13].

Hydrotreating catalysts contain metals dispersed on support, while stability, proper performance, and enough surface area for dispersion of active sites in catalysts are provided by supports[14]. Alumina, silica, zeolites, carbon structures, and zirconia have been used in hydrodesulfurization catalyst fabrication [15]. Molybdenum sulfide supported on  $\gamma$ -alumina catalysts with Ni and Co promoters are among the most studied catalysts and have been widely used in industrial HDS processes[16–18]. The sulfided NiMo- $\gamma$ -alumina catalysts have been designed for hydrodesulfurization but are also used for hydrogenation and hydrodenitrogenation[19,20]. Economic and environmental issues have always been considered in catalyst developing and using in industries. In this regard, active carbon has attracted attentions to be used as a novel economic and environmentally friendly support for industrial catalysts [21].

Activated carbon can be synthesized through chemical or physical activation methods [22]. The carbonization of a carbonaceous precursor is the central part of the resulting bio-char. In physical activation, the resulting bio-char is activated using activating agents such as carbon dioxide or steam[23,24]. Chemical activation can be performed in a single step, which is the precursor's carbonization in the presence of many different chemical agents such as  $ZnCl_2$ , KOH, etc. The lower activation temperature and as a result the less energy consumption, higher yield and porosity and less time for activation are essential advantages of the chemical activation method[25,26].

Activated carbon as a precious metal catalyst carrier with small metal-support interaction, low coke formation, and high metal recovery potential from the spent catalysts has been reliable support for HDS reactions [27].

Compared with alumina, carbon supports have fewer polarities, enhancing the dispersion of Mo active metal and Ni or Co promoter on the support with less interaction between the support and dispersed metals[28]. Hydrodesulfurization of gas oil using NiMo catalysts, supported on activated carbon exhibited higher activity and acceleration for the HDS of 4,6-DMDBT than a commercial NiMo-Alumina catalyst[29,30]. The same was reported for using NiMo-sulfides or CoMo-sulfides on active carbon in HDS of dibenzothiophene (DBT) or its alkyl-derivatives [31].

Different biomasses, mainly agricultural wastes such as walnut and coconut shells, with high carbon content can be converted to active carbon in a relatively simple process and low cost per cubic meter [32,33]. Thermal treating and activation process makes randomized bonding, high porosity, numerous cracks and voids between the carbon layers and great internal surface area in active carbon structure. This makes micro and meso structure for carbonaceous catalyst supports, while mesoporosity gives benefits in terms of available surface area for catalyst dispersion[34]. Besides, expensive metals used as active phase in carbon-based support catalysts can be easily recovered from used catalysts by burning the carbon support [19]. This is while that expensive and complicated methods such as leaching, selective precipitations and solvent extraction are the most used recycling experiment for alumina and silica-based supports [35].

In this work, walnut shell as agricultural waste and source of carbonaceous material was chemically activated with zinc chloride. The walnut active carbon (WAC) was functionalized with  $HNO_3$  and  $H_2SO_4$  and used as support for NiMo catalyst synthesis. NiMo-WAC nanocatalysts' catalytic activities were evaluated under different operating conditions and functionalization with  $HNO_3$  compared with commercial catalyst. The main novelties are as follows:

- Synthesis of a novel, environmentally friendly functionalized active carbon, used as a catalyst support with high dispersion of Mo active metal and Ni promoter on its surface area.
- High activity of synthesized NiMo catalysts supported on functionalized active carbon for heavy naphtha hydrotreating in comparison with common industrial hydrotreating catalysts.

## EXPERIMENTAL SECTION

### Materials

Walnut shell as agricultural waste was collected from walnut gardens in Yasuj city of Iran to produce active carbon as catalyst support. Ammonium heptamolybdate tetrahydrate  $(\text{NH}_4)_6\text{Mo}_7\text{O}_{24}\cdot 4\text{H}_2\text{O}$ , nickel nitrate hexahydrate  $\text{Ni}(\text{NO}_3)_2\cdot 6\text{H}_2\text{O}$ , zinc chloride  $\text{ZnCl}_2$ , nitric acid 67%, sulfuric acid 98.8% and hydrochloric acid 37%, all were purchased from Sigma-Aldrich, also  $\text{NiMo}-\gamma\text{Al}_2\text{O}_3$ , dimethyl disulfide (DMDS, Merck), deionized water (DI), and analytical grade  $\text{H}_2$  were used in the experiments.

### Preparation of active carbon

Walnut shell samples were washed with deionized water, dried in the oven at  $105^\circ\text{C}$  for 2 h, crushed, and sieved to a particle size of 0.85-1 mm to be used for support preparation. The meshed walnut shell particles and zinc chloride pellets (with the weight ratio of 5:1) were mixed with deionized water in an Erlenmeyer flask and refluxed for 6 h in  $80^\circ\text{C}$ . The Erlenmeyer flask's content was filtered, dried at  $60^\circ\text{C}$  for 5 h and pyrolyzed in a vertical reactor at  $500^\circ\text{C}$  for 1 h. The solid product of pyrolysis (bio-char) was washed with 0.1 M HCl for 1 h in  $80^\circ\text{C}$  and dried for 5 h at this temperature. To functionalize the obtained active carbon, it was refluxed with 4M  $\text{HNO}_3$  and  $\text{H}_2\text{SO}_4$  in  $80^\circ\text{C}$  for 7 h and then filtered and dried in  $80^\circ\text{C}$  for 5 h. The synthesized active carbon and treated active carbon samples with  $\text{HNO}_3$  and  $\text{H}_2\text{SO}_4$  were named WAC1, WAC2, and WAC3 respectively and were used as catalyst support[26].

### Preparation of catalysts

The method of incipient wetness impregnation was used to prepare three catalysts of NiMo supported on the WAC1, WAC2, and WAC3. Each support was loaded by a certain amount of the molybdenum using aqueous solutions containing  $(\text{NH}_4)_6\text{Mo}_7\text{O}_{24}\cdot 4\text{H}_2\text{O}$  and  $\text{Ni}(\text{NO}_3)_2\cdot 6\text{H}_2\text{O}$ . NiMo-WAC1, NiMo-WAC2. To this, a certain amount of dried functionalized active carbon was dipped into a beaker containing the as-prepared solutions in 10 mL deionized water, with the aim of 12 %wt. and 3 %wt. Mo and Ni impregnation. The mixture was stirred for approximately 120 min at  $60^\circ\text{C}$  and then was left in room temperature, overnight. The impregnated materials were calcined in argon flow at  $550^\circ\text{C}$  for 3 h and then were slightly exposed to the atmosphere during

the cooling procedure and the synthesized catalysts, using walnut active carbon supports functionalized with HCl,  $\text{HNO}_3$  and  $\text{H}_2\text{SO}_4$  were named NiMo-WAC1, NiMo-WAC2 and NiMo-WAC3 respectively.

### Characterization

Elemental analyses were performed to identify the walnut shells' constituent elements using CHNS (Eager 300 for EA1112), and the oxygen content was ascertained by difference on a dry ash-free basis[36]. The walnut shell sample's moisture and volatile content were obtained using a thermogravimetric analyzer (SDTA851 and METTLER-TOLEDO compact) with the temperature program of 30 to  $800^\circ\text{C}$ , the heat rate of  $10^\circ\text{C}/\text{min}$  and  $\text{N}_2$  gas flow of 20 L/min. The standard test method for determining the biomass' ash content, ASTM E1755, was used to determine the sample ash content and the fixed carbon calculated by difference. The pyrolysis of the impregnated walnut shell with  $\text{ZnCl}_2$  in  $500^\circ\text{C}$  resulted in 48% bio-char, 47% bio-oil, and 5% gas.

To study the physicochemical properties of the catalysts FESEM analysis (FESEM, MIRA III, TESCAN, Czech Republic) was conducted. Using XRD, Philips PW1840 X-ray diffractometer the patterns of the calcined catalysts was studied. As a repeatable and reliable technique, ICP (Varian VISTA-MPX) analysis was performed to measure metal loadings of the catalysts. The specific surface area, average pore volume, and average pore diameters of the support and catalysts were measured by BET surface area analysis, via an ASAP-2010 V2 Micrometrics TriStar II Plus 2.03 system. To identify functional groups over synthesized catalysts, FT-IR was conducted on Bruker ISS-88 FTIR spectroscopy instruments in a spectrum range from 400 to  $4000\text{ cm}^{-1}$ . To determine the distribution of acid sites on synthesized catalysts,  $\text{NH}_3$ -TPD analysis was performed using Chemisorption Analyzer, Nanos ORD made by Sensiran Co., Iran. To measure total sulfur content of the oils, X-ray fluorescence spectrometry technique (XRF, Tanaka scientific sulfur meter model RX-360SH) was used. Metal reducibility was studied with TPR technique, in a Micromeritics AutoChem 2920 apparatus.

### Catalytic activity in hydrodesulfurization

The hydrodesulfurization reactions were carried out in a continuous down-flow fixed-bed stainless steel reactor

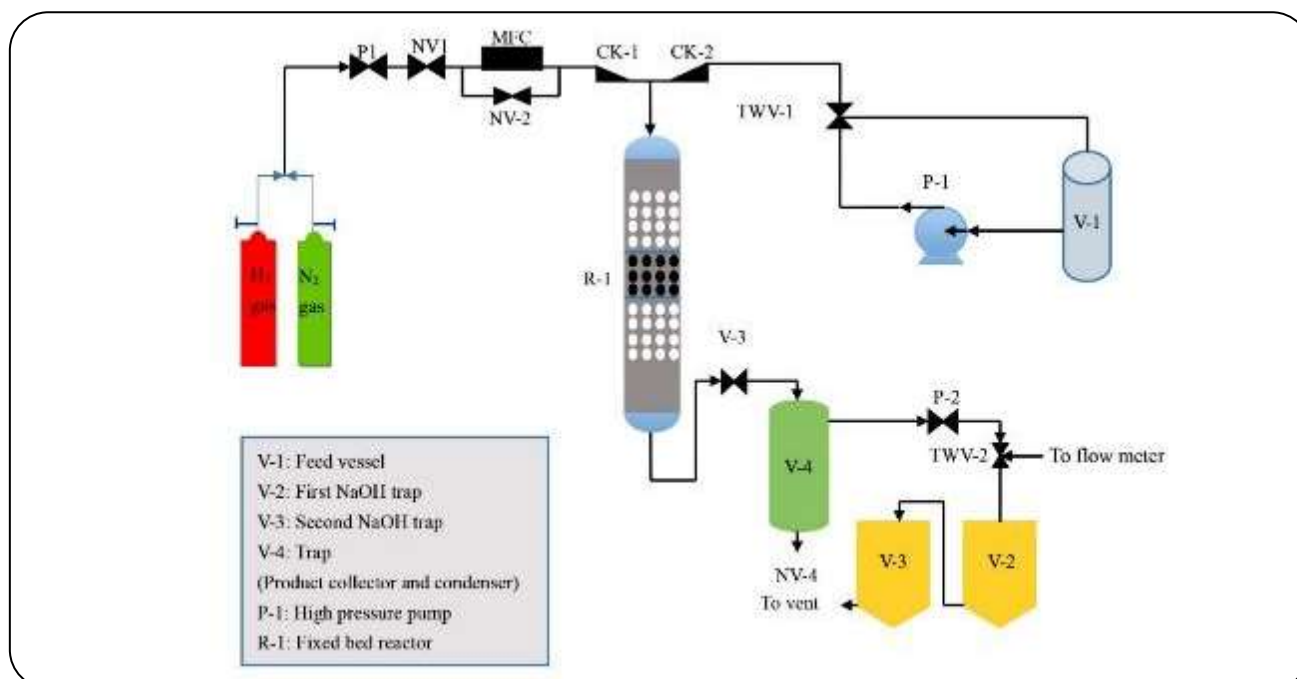


Fig. 1: Schematic diagram of the reactor setup.

with the inner diameter and length of 10 mm and 450 mm, respectively, heated in a three-zone furnace. The experimental reactor setup schematic and feed characterization result are shown in Fig. 1 and Table 1. For each test, 1 g of the synthesized catalyst was charged into the reactor's central segment between two layers of glass beads and carborundum filler. Nitrogen gas was used to carry out a leak test, and then the gas was shifted to hydrogen. To activate catalysts, dimethyl disulfide (DMDS) was injected into the reactor in two steps: the first in low temperature of 220 °C for 4 hours and the second in high temperature of 330 °C for 12 h duration which for both the pressure, LHSV and  $H_2/oil$  were set at 30 bar,  $3.3h^{-1}$  and 100 NL/L respectively. Heavy naphtha as the feedstock in assessing the prepared catalysts in HDS reaction was added to the reactor using an HPLC pump (KNAUER K-501) and mixed with  $H_2$  injected into the reactor by Brooks 5850 mass flow controller (MFC). The reactor's temperature was increased with the electric furnace to desired temperatures defined in Table 1. The product was continuously gathered in a condenser with temperature 40 °C. The collected treated products were used for sulfur measurements. Exited gases from condenser were trapped in the NaOH solution and the remaining gases were sent to vent. The specific catalytic activity for the HDS reaction was studied in different operation

variables such as LHSV,  $H_2/oil$ , reaction temperature and pressure. Finally, products were gathered in the condenser and were drained after each 24 h. Then the final sulfur contents of liquid product were analyzed by XRF technique. The properties of heavy naphtha feed and operational conditions for the HDS reaction are illustrated in Table 1.

## RESULTS AND DISCUSSION

### Characterizations

The proximate analysis results of the walnut shell (W) and the elemental composition of walnut shell (W) and Walnut shell Activated Carbon (WAC), in as received and dry ash-free(daf) basis, are listed in Table 2. It can be seen that carbonization and activation of walnut shells increased carbon content in WAC, while the contents of hydrogen and oxygen decreased.

High carbon and low ash content are the positive characteristics for choosing walnut shell biomass to produce active carbon [37]. Besides, the negligible amount of nitrogen and no sulphur in walnut shell samples was a good sign for less emission of toxic compounds such as  $SO_x$  and  $NO_x$  during the feed carbonization through pyrolysis[38]. According to Table 2 and also Fig. 2 the volatile matters in the walnut shell sample of this study was high and in the range of many other walnut shell

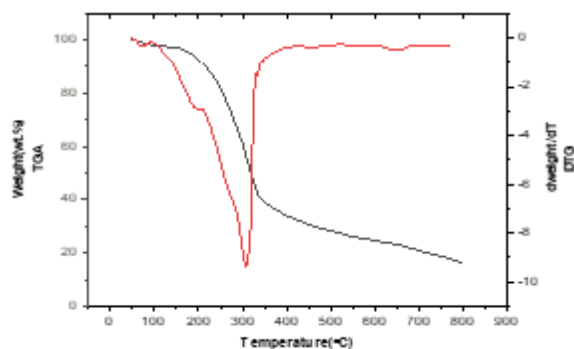
**Table 1: Properties of heavy naphtha feed in this study.**

Total sulfur (mg/L)	2491
Density at 15.56 °C (g.cm <sup>-3</sup> )	727±0.001
Boiling range (°C)	ASTMD86
IBP	50.3±0.01
T <sub>5%</sub> (°C)	60.3±01
T <sub>10%</sub> (°C)	67.5±01
T <sub>20%</sub> (°C)	78.6±01
T <sub>30%</sub> (°C)	87 ±01
T <sub>40%</sub> (°C)	96.1±01
T <sub>50%</sub> (°C)	104.8±01
T <sub>60%</sub> (°C)	118.1±01
T <sub>70%</sub> (°C)	131.4±01
T <sub>80%</sub> (°C)	150.7±01
T <sub>90%</sub> (°C)	189.6±01
FBP	233.7±01

**Table 2: Proximate analysis of W and Elemental analysis of W and WAC.**

	Proximate analysis (wt.%)		Elemental analysis (wt.%, daf**)		
	W		W	W	WAC
Volatile matter	78.4		C	49.7	55.3
Fixed Carbon	20.2		H	6.5	5.0
Ash	0.8		N	0.3	0.5
Moisture	0.6		O*	43.5	39.2

\*Calculated by  $O\% = 100\% - C\% - H\% - N\% - S\%$  on a daf basis. \*\* daf, dry ash-free basis

**Fig. 2: Walnut shell TGA-DTG.**

samples used in other researches [39,40] since the escape of volatile matter facilitates the occurrence of pyrolysis [38] in carbonization step. According to thermogravimetry (TGA) and differential thermogravimetry (DTG) curves of walnut shell (Fig. 2), the feedstock decomposition occurs in three steps. First step of TGA curve (from 50 to 200 °C), can be attributed to water and slight volatile release. The maximum mass loss happens in the second step from 200 to 400 °C. The third zone starts at around 400 °C and continues to 800 °C, and it is seen as a tailing in both TGA and DTG curves[36,39]. Walnut shell is mainly composed of hemicellulose, cellulose, and lignin like all other lignocellulosic materials. According to the thermogravimetric behavior of individual components, hemicellulose, cellulose, and lignin complete their decomposition at temperature intervals of 210–325, 310–400, and 160–900 °C, respectively[39]. Based on these information, the minor and major reactions observed in active pyrolysis zone can mainly be attributed to hemicellulose and cellulose decomposition, respectively [39].

FESEM micrographs of nanocatalyst samples, NiMo-WAC1, WAC2, and WAC3, are shown in Fig. 3 with magnifications of 200 nm. The results indicated that no visible gross particles were seen in the NiMo-WAC nanocatalysts. The surface seemed to be covered with a lot of tiny nanoscale particles. Pretreating WAC with HCl, HNO<sub>3</sub>, and H<sub>2</sub>SO<sub>4</sub> caused partial damage in the feed structure, and some morphological changes were seen. As a result, the samples' surface porosity was increased, although their main framework was unchanged.

Treatment with HNO<sub>3</sub> has decreased particles' size (Fig. 3b), which yielded thin flakes and a more porous structure. This made metal ions spread and diffusion much more comfortable, and as a result, a catalyst with suitable and stable active sites and high yielded desulfurization was synthesized [14].

The crystal phases of all the catalysts were examined by X-Ray Diffraction (XRD) powder analysis, and the results are illustrated in Fig. 4. The sulfide catalyst (NiMoS-WAC1) XRD patterns were compared with reference MoS<sub>2</sub>. The peaks at  $2\theta = 33$  and  $58.5$  are assigned to (100) and (110) lattice planes of the MoS<sub>2</sub> phase (JCPDS card No. 75-1539), and this confirms the MoS<sub>2</sub> crystalline nature (Fig. 4)[41]. Also, the peak at  $2\theta = 38^\circ$  is assigned to the (220) of NiS (JCPDS No. 12-0041). The diffraction peak at about  $2\theta$  value of  $25^\circ$  is prominent

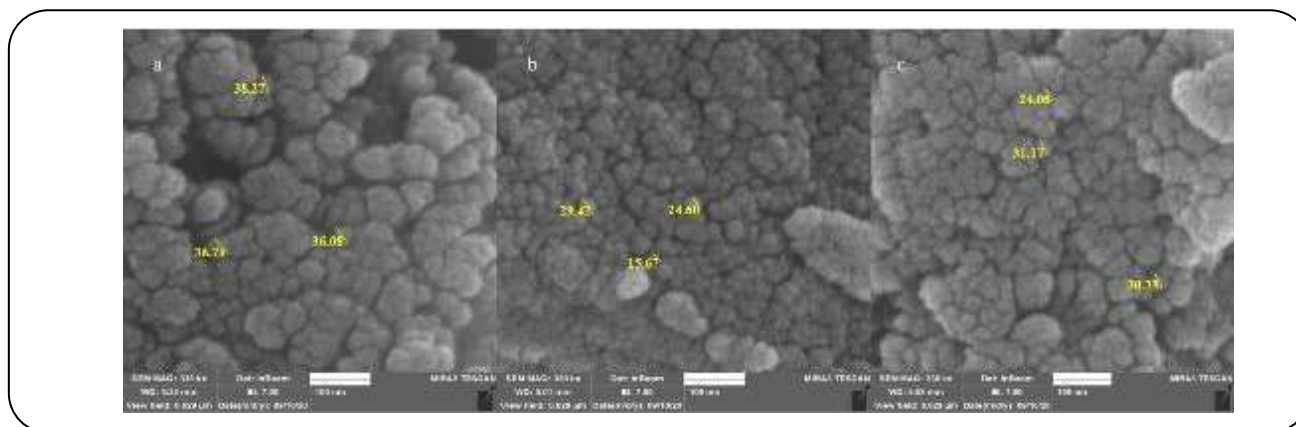


Fig. 3: FESEM images (a) NiMo-WAC1, (b) NiMo-WAC2, and (c) NiMo-WAC3.

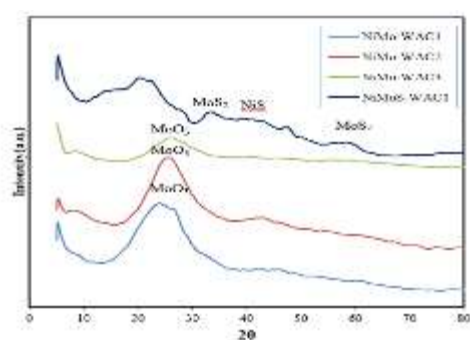


Fig. 4: XRD patterns of NiMo-WAC nanocatalysts: (a) NiMo-WAC1, (b) NiMo-WAC2, (c) NiMo-WAC3, (d) NiMoS-WAC1.

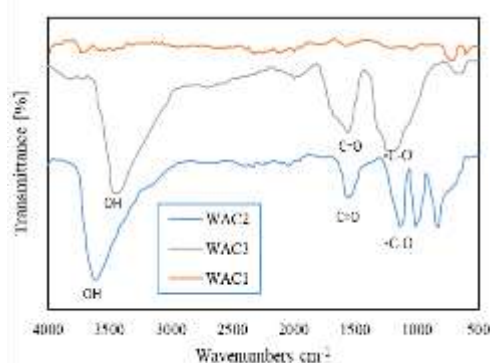


Fig. 5: FT-IR spectrum of WAC1, WAC2, and WAC3.

catalysts which can be assigned to the hexagonal  $\text{MoO}_3$  or graphite[42]. This is while that the peaks at  $2\theta$  of  $20 - 30^\circ$  (002)  $40 - 50^\circ$  (101) have been announced as the graphite phase of active carbon [19]. The extra peaks can be assigned to other forms of molybdenum oxide similar to  $\text{MoO}_2$  or  $\text{MoO}_3$ . Consequently, these peaks' attendance can be considered a further indication of the AC's successful impregnation with the metal catalyst. Mo-oxides' presence causes a significant blockage of the pores of the activated carbon support [9].

FT-IR spectra for the synthesized catalysts support indicating the surface functional groups are shown in Fig.5. In absorption bands of WAC1 support, it has established 701 and 3733  $\text{cm}^{-1}$  bands assigned to C=O, and O-H groups, respectively. Strengthening functional groups and their higher quantities in the nitric and sulfuric acid-treated carbon supports (WAC2 and WAC3) is evident in comparison with WAC1. Absorption bands centered at about 3400-3700  $\text{cm}^{-1}$  in WAC2 and WAC3 are related

to the stretching vibrations of individual O-H bands. Two catalyst support of WAC2 and WAC3 also have peaks around 1700  $\text{cm}^{-1}$  which can be related to C=O stretching vibrations of carboxylic and carbonyl compounds. The bands around 1100-1200  $\text{cm}^{-1}$  in these supports are assigned to -C-O stretching groups. [43][44].

According to the IUPAC class, the  $\text{N}_2$  adsorption-desorption isotherms of the calcined catalysts were observed to be type-IV with some hysteresis (Fig. 6).

Table 3. shows the percent and ratio of Ni and Mo impregnated on support. In this table surface area, pore-volume, and pore diameter of synthesized WAC, NiMo-WAC1, NiMo-WAC2, and NiMo-WAC3 were demonstrated and compared with NiMo- $\gamma\text{-Al}_2\text{O}_3$ . The functionalization of supports made a higher surface area and pore volume than walnut active carbon(WAC) due to the presence of defects after functionalization[45]. This has increased mesoporosity and significant hysteresis in the adsorption/desorption diagram of the related

**Table 3. Metal contents, BET surface areas, total pore volumes, and average pore sizes of walnut active carbon (WAC) and synthesized catalysts.**

Catalyst	Mo (wt.%)	Ni (wt.%)	Ni/Mo	Total metal	Specific surface area(m <sup>2</sup> /g)	Pore volume(cm <sup>3</sup> /g)	Pore size (nm)
WAC	0	0	0	0	1621	1.51	3.20
NiMo-WAC1	11.38	2.67	0.235	14.05	827	0.79	3.60
NiMo-WAC2	11.42	2.71	0.237	14.13	768	0.67	5.20
NiMo-WAC3	11.40	2.67	0.234	14.07	725	0.61	5.40
NiMo- $\gamma$ -Al <sub>2</sub> O <sub>3</sub>	11.40	2.70	0.236	14.10	216.5	0.54	6.50

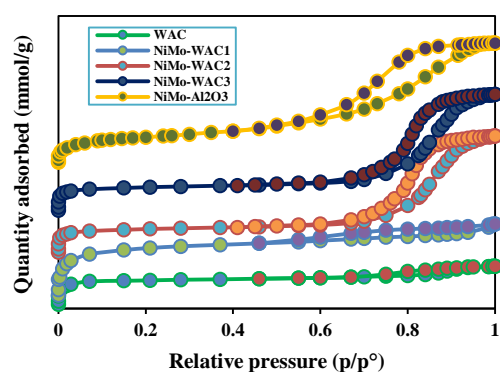


**Fig. 6: Nitrogen adsorption-desorption isotherms measured ( $T=77K$ ).**

catalysts (NiMo-WAC2 and NiMo-WAC3 in Fig. 6). The surface area and pore volume of the synthesized catalysts were smaller than that of the Walnut shell Activated Carbon (WAC). The pore diameters were increased as active metal sites blocked micropores. [46].

The acidity of the catalysts was characterized through Temperature Programmed Desorption of ammonia (NH<sub>3</sub>-TPD) as a useful tool. As it can be seen in Fig. 7, determination of the catalysts' acidity was sequentially assigned to the peak regions of NH<sub>3</sub>-TPD curves where below 350°C a peak and in 350-600°C the rest of the peaks were observed. This confirmed the weak and medium acidity of the catalysts [47,48]. NiMo-WAC2 exhibited a peak at 526°C, a strong acid site and straightly related to hydrogenation activity and higher conversion in desulfurization [49].

The interaction of the Ni and Mo metallic phases with the AC support was studied with TPR analysis. As it can be seen in Fig. 8 all three catalysts showed a main reduction peak between 300 to 450 °C, while NiMoAC2 catalyst has showed the peak at 344 °C and NiMoAC3 and NiMoAC1 at temperatures of 370 and 385 °C respectively during the reduction process[50].

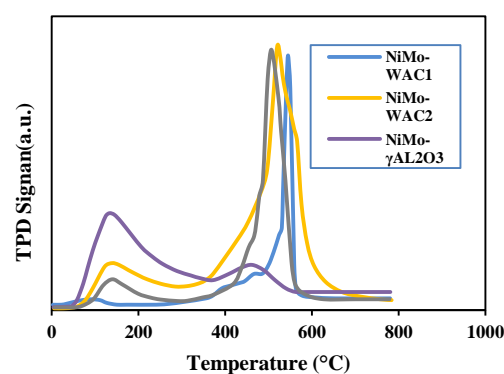


**Fig.7: NH<sub>3</sub>-TPD Result of the NiMo-WAC1, WAC2, WAC3, and NiMo- $\gamma$  Al<sub>2</sub>O<sub>3</sub>.**

The high temperature peaks reduction signal between 550 and 600 °C observed in the TPR of all the catalysts could be assigned to reduction of the carbon support[51].

To check reusability of the synthesized catalysts, three catalysts of NiMoWAC1, NiMoWAC2 and NiMoWAC3 were tested in individual reactions for five consequence cycles. Fig.9. shows the sulfur removal of the heavy naphtha feed in mentioned five cycles. Each test was held at 300 °C for 5 h. The least activity loss was observed for NiMo-WAC2 catalyst after five cycles, indicating the remarkable reusability of this catalyst.

#### **The activity of catalysts in the hydrodesulfurization process**

The HDS activities of walnut active carbon-supported catalysts were studied for heavy naphtha with many sulfur compounds (about 70%), including thiophene and condensed-ring thiophenes as DBT. Some other types of sulfur compounds in the heavy naphtha are sulfides and mercaptans, critical to being removed as environmental pollutant sources[52]. The reaction network's main pathways for DBT hydrodesulfurization are illustrated in Fig. 10

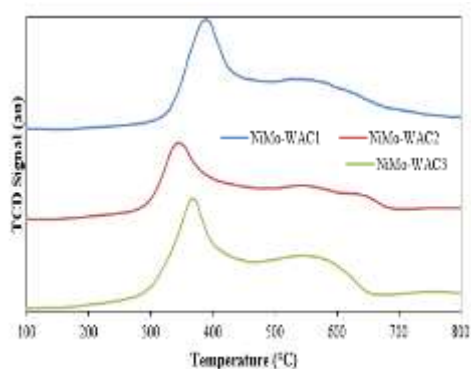


Fig. 8: TPR profiles of the fresh catalysts.

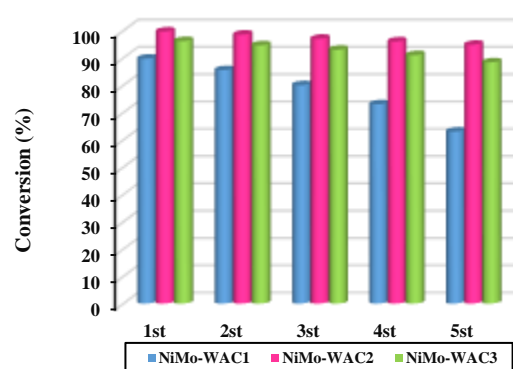


Fig. 9: Sulfur removal of the heavy naphtha for five consecutive cycles.

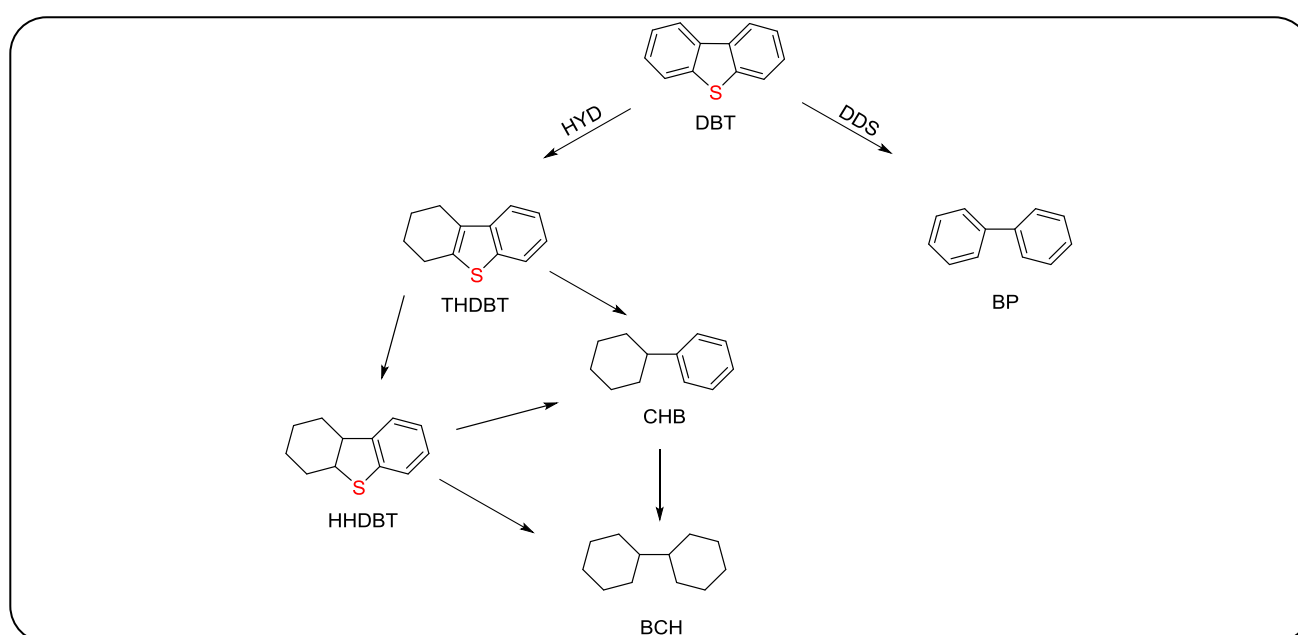


Fig. 10: Two main pathways of reaction network for DBT hydrodesulfurization (hydrogenation (HYD) and direct desulfurization (DDS)).

as hydrogenation (HYD) and direct desulfurization (DDS). In the HYD pathway, the first hydrogenated DBT transforms to tetrahydro dibenzothiophene (THDBT) or hexahydro dibenzothiophene (HHDBT) and then is formed cyclohexylbenzene (CHB) and bicyclohexyl (BCH)[31].

The NiMo-WAC2 catalyst with porous structure could provide further active sites for the reaction and usually went through the DDS pathway in Hydrodesulphurization of DBT with high performance in hydrodesulphurization [53]. In this experiment, the HDS degrees of heavy naphtha over NiMo-WAC2 and NiMo- $\gamma$ -Al<sub>2</sub>O<sub>3</sub> (commercial) catalysts at different operational conditions of pressures, temperatures,

LHSV ratios were tested, which in all the tests, one parameter was changed, and the other parameters stayed constant. The results are shown in Fig.11.

To optimize operational conditions of the NiMo-WAC2 catalyst as a catalyst with strong acid sites and porous structure and high surface area, the effect of temperature, pressure, LHSV, H<sub>2</sub>/oil ratio and time as operating conditions affecting sulfur removal of the considered heavy naphtha feed were tested, and the results are illustrated in Fig.11. All parameters took near industrial conditions. The percentage of potential experimental error was about 2%–3% for all samples, demonstrated in Fig. 11 by error bars.

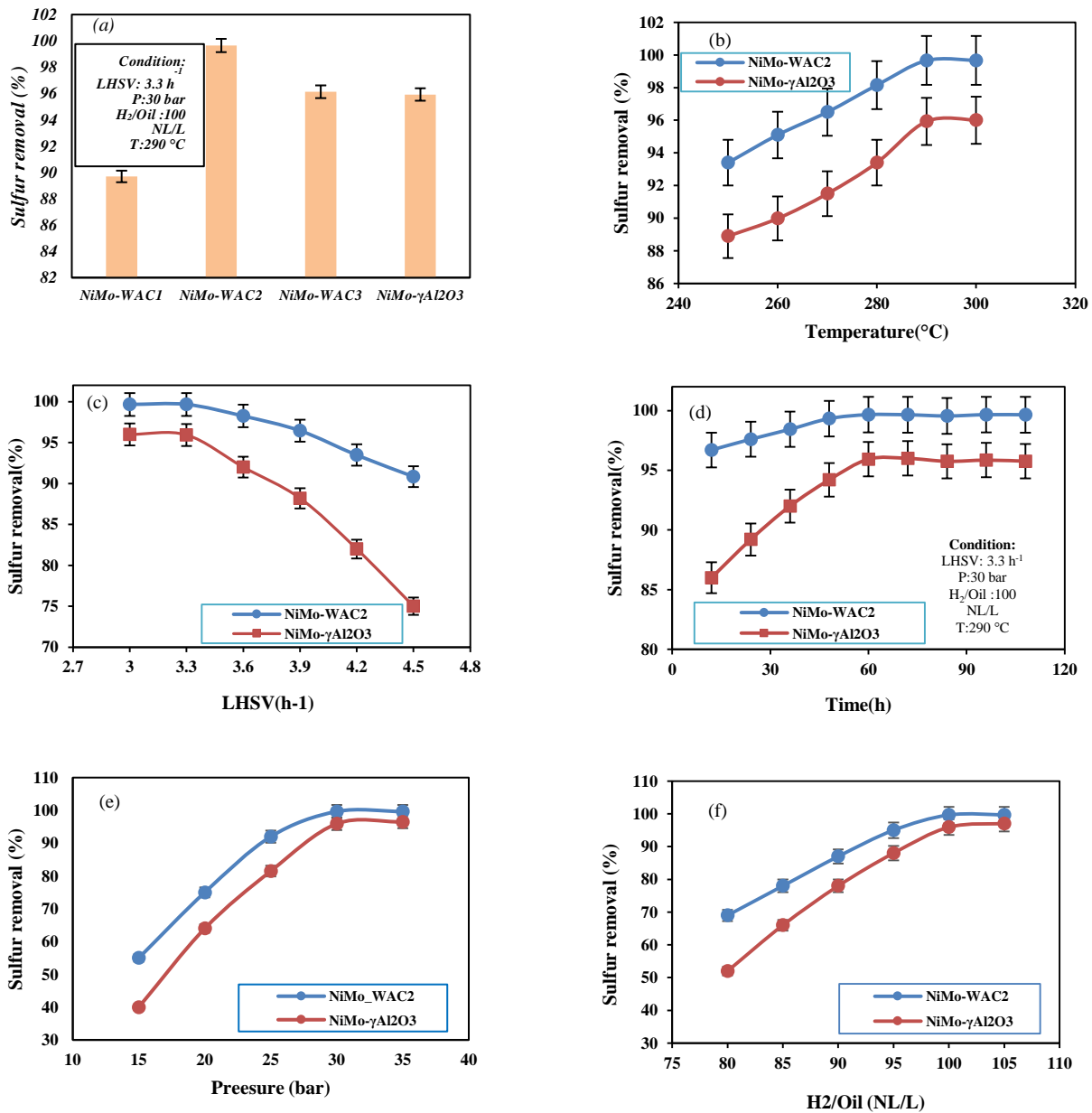


Fig. 11: HDS conversion of heavy naphtha. (a) catalysts performance comparison Effect of (b) Temperature, (c) LHSV, (d) Time, (e) Pressure, and (f) H<sub>2</sub>/oil on sulfur removal.

The performance of the NiMo-WAC1, NiMo-WAC2, NiMo-WAC3 and NiMo- $\gamma$ Al<sub>2</sub>O<sub>3</sub> as an industrial catalyst in sulfur removal is illustrated in Fig. 11 (a). It is evident in this figure that the maximum efficiency in sulfur removal for heavy naphtha is for NiMo-WAC2 and NiMo- $\gamma$ Al<sub>2</sub>O<sub>3</sub> catalyst at 290°C, with better performance of NiMo-WAC2 catalyst in the sulfur removal from heavy naphtha. All catalysts showed an enhancement in catalytic activity as a function of temperature. The performance

of the catalysts followed the trend of NiMo-WAC2 > NiMo-WAC3 > Ni-Mo/ $\gamma$ Al<sub>2</sub>O<sub>3</sub> > NiMo-WAC1 at temperatures of 290°C.

As shown in Fig.11 (b), The temperature effect was evaluated in the range of 250 to 300 °C while other parameters, including pressure at 30 bars, LHSV at 3.3 h<sup>-1</sup> and H<sub>2</sub>/feed at 100 NL/L were constant. According to this figure, sulfur removal percent increased with enhancing the temperature. By temperature increase, heteroatoms

**Table 4: Oil, gas, and coke yields after HDS process gas in conditions of  $T=290\text{ }^{\circ}\text{C}$ ,  $P=30\text{ bar}$ ,  $LHSV=3.3\text{ h}^{-1}$ ,  $H_2/Oil=100\text{ NL/L}$ .**

Experiment	Liquid (wt. %)	Gas (wt. %)	Coke (wt. %)
Upgrading heavy naphtha	$97.51 \pm 1.11$	$2.34 \pm 1.22$	$0.15 \pm 0.12$

remove faster while the activity of the catalysts decrease as a result of reactants cracking and products coking[54].

As displayed in Fig. 11 (c), with changing LHSV from 3 to  $4.5\text{ h}^{-1}$  the sulfur removal percent changed, and the most suitable LHSV value for NiMo-WAC2 catalyst was  $3.3\text{ h}^{-1}$ . Also, according to Fig. 11(d), the HDS conversion for NiMo-WAC2 and Ni-Mo/ $\gamma\text{-Al}_2\text{O}_3$  under constant operating conditions is a function of time for fresh catalyst, and after 108 h, the catalyst retains its sustainability.

To study the pressure effect on sulfur removal from the feed, the tests were repeated in five points from 15 to 35 bar while the rest of the parameters were constant, and the results are shown in Fig. 11 (e). According to the results, NiMo/WAC2 at the pressure of 30 bar with a temperature of  $290\text{ }^{\circ}\text{C}$  and  $LHSV\ 1\text{ h}^{-1}$  reached the maximum sulfur removal from heavy naphtha.

Also, from Fig. 11 (f), it is evident that in the various LHSV ( $3\text{-}4.5\text{ h}^{-1}$ ), with the increase in the ratio of  $H_2/oil$ , sulfur removal from the feed increased. The most suitable ratio for NiMo-WAC2 catalyst was 100 NL/L.

From Fig. 11 (a), it can be seen that more than 99.66 % of the feed's sulfur components were eliminated in the product by NiMo-WAC2 catalyst in optimum conditions of LHSV, pressure,  $H_2/Oil$ , and temperature [48]. The higher activity of NiMo-WAC2 catalyst than the supported commercial catalyst in desulfurization process can be related to strong acid sites, porous structure and high surface area of the synthesized support. This caused high dispersion of NiMo metal phase on the support and more active sites for reactions resulted extraordinary performance in desulfurization process.

Table 4 displays the gas, liquid, and coke's mass balance after heavy naphtha upgrading under  $H_2$  gas. These values confirm that NiMo-WAC2 catalyst suppressed undesired coking reactions and subsequently increased heavy molecular weight hydrocarbons' conversion to light products.

The gas chromatography (GC) method was used to determine the compounds in the exhaust gas. The GC test results obtained from the exhaust gas in the upgrading conditions are summarized in table 5.

**Table 5: Produced gas composition of heavy naphtha for HDS process in conditions of  $T=290\text{ }^{\circ}\text{C}$   $p=30\text{ bar}$ ,  $LHSV=3.3\text{ h}^{-1}$   $H_2/Oil=100\text{ NL/L}$ .**

Compound	Percentage (Vol. %)
$H_2$	$70.882 \pm 0.001$
$H_2S$	$0.004 \pm 0.001$
$NH_3$	$0.006 \pm 0.001$
$N_2$	$0.003 \pm 0.001$
$CH_4$	$17.212 \pm 0.001$
CO	$0.120 \pm 0.001$
$CO_2$	$0.161 \pm 0.001$
$C_2^+$	$11.612 \pm 0.001$
Total	100

In Table 6 the performance of NiMo-WAC2 with some other catalysts in hydrodesulphurization process of heavy naphtha in similar conditions has been compared. It is evident that NiMo-WAC2 with high conversion can be a good selection in naphtha HDS.

## CONCLUSIONS

In this research, the walnut shell active carbon (WAC) was synthesized through chemical activation. Functionalized active carbons with HCl,  $HNO_3$ , and  $H_2SO_4$  were used as support for NiMo hydrodesulfurization catalysts synthesis and were named NiMo-WAC1, NiMo-WAC2, and NiMo-WAC3. These catalysts were thoroughly characterized through FT-IR, XRD, ICP, BET-BJH, FESEM,  $NH_3$ -TPD and TPR techniques.

Brilliance characteristics such as a considerably increasing porous structure, a high degree of total acidity and the high surface area created more active sites and better dispersion of NiMo metal phases on the synthesized supports of catalysts. The catalysts were used for the HDS reaction on the heavy naphtha feed with a total sulfur content of 2491 ppm under operating conditions of  $T = 290\text{ }^{\circ}\text{C}$ ,  $LHSV = 3.3\text{ h}^{-1}$ ,  $P = 30\text{ bars}$ , and  $H_2/feed = 100\text{ NL/L}$ . The NiMo-AC2 catalyst showed 99.6 wt.% conversion in hydrodesulphurization of the naphtha feed which

Table 6. NiMo-WAC2 synthesized catalyst vs. some studied experiments

Catalyst	Feed	Op.Con	HDS	ref
NiMo/NG	heavy naphtha	290 °C 30 bar	99.5%	[55]
Ni-Mo/ $\gamma$ -alumina	heavy naphtha	290 °C 3 MPa	95%	[56]
NiMo -amine-functionalized graphene	heavy naphtha	290 °C 3 MPa	97.8%	[57]
NiMo-WAC2	heavy naphtha	290 °C 30 bar	99.66	The present Work

was considerably more than commercial NiMo- $\gamma$ Al<sub>2</sub>O<sub>3</sub> catalysts.

Received : Nov. 6, 2021 ; Accepted : Feb. 14, 2022

## REFERENCES

- [1] Abubakar U.C., Alhooshani K.R., Saleh T.A., Effect of Ultrasonication and Chelating Agents on the Dispersion of Nimo Catalysts on Carbon for Hydrodesulphurization., *J. Environ. Chem. Eng.*, **8**: 1–6 (2020).
- [2] Padervand M., Rhimi B., Wang C., One-pot Synthesis of Novel Ternary Fe<sub>3</sub>N/Fe<sub>2</sub>O<sub>3</sub>/C<sub>3</sub>N<sub>4</sub> Photocatalyst for Efficient Removal of Rhodamine B and CO<sub>2</sub> Reduction, *J. Alloys Compd.*, 852 (2021).
- [3] Padervand M., Lammel G., Bargahi A., Mohammad-Shiri H., Photochemical Degradation of the Environmental Pollutants over the Worm-Like Nd<sub>2</sub> CuO<sub>4</sub> -Nd<sub>2</sub>O<sub>3</sub> Nanostructures, *Nano-Structures and Nano-Objects*, **18**: 100258 (2019).
- [4] Padervand M., Gholami M.R., Removal of Toxic Heavy Metal Ions from Waste Water by Functionalized Magnetic Core-Zeolitic Shell Nanocomposites as Adsorbents, *Environ. Sci. Pollut. Res.*, **20**: 3900–3909 (2013).
- [5] Heidari Samiromi A., Jahangiri A.R., Investigation of CO<sub>2</sub> Solubility in Blends of AMP and HMDA Solvents: Thermodynamic Modeling Based on the Deshmukh-Mather Model, *Iran. J. Chem. Chem. Eng. (IJCCE)*, **40**(1): 231–240 (2021).
- [6] Alinezhad H., Fakhimi Abarghouei M.R., Tajbakhsh M., Niknam K., Application of Mea, Tepa, and Morpholine Grafted Nay Zeolite as CO<sub>2</sub> Capture, *Iran. J. Chem. Chem. Eng.*, **40**(2): 581–592 (2021).
- [7] Baradaran S, Sadeghi M.T., Desulfurization of Non-Hydrotreated Kerosene Using Hydrodynamic Cavitation Assisted Oxidative Desulfurization (HCAOD) Process, *J. Environ. Chem. Eng.*, **8**: 103832 (2020).
- [8] Ebrahiminejad M., Karimzadeh R., Hydrocracking and Hydrodesulfurization of Diesel Over Zeolite Beta-Containing NiMo Supported on Activated Red Mud, *Adv. Powder. Technol.*, **30**: 1450–1461 (2019).
- [9] Sheibani S., Zare K., Mousavi Safavi S.M., The Effects of pH and Chelating Agent on Synthesis and Characterization of NI mo/ $\gamma$ - Alumina Nanocatalyst for Heavy Oil Hydrodesulfurization, *Iran. J. Chem. Chem. Eng. (IJCCE)*, **40**(1): 21–34 (2021).
- [10] Yin C., Wang Y., Effect of Sulfidation Process on Catalytic Performance over Unsupported Ni-Mo-W Hydrotreating Catalysts, *Korean. J. Chem. Eng.*, **34**: 1004–1012 (2017).
- [11] Gao Q., Ofosu T.N.K., Ma S.G., Komvokis V.G., Williams C.T., Segawa K., Catalyst Development for Ultra-Deep Hydrodesulfurization (HDS) of Dibenzothiophenes. I: Effects of Ni Promotion in Molybdenum-Based Catalysts, *Catal. Today*, **164**: 538–543 (2011).
- [12] Kokayeff P., Zink S., Roxas P., "Hydrotreating in Petroleum Processing", Handbook of Petroleum Processing, pp. 1-59 (2015).
- [13] Mahmoudabadi Z.S., Rashidi A., Tavasoli A., Synthesis of Two-Dimensional TiO<sub>2</sub>@ Multi-Walled Carbon Nanotube Nanocomposites as Smart Nanocatalyst for Ultra-Deep Oxidative Desulfurization of Liquid Fuel: Optimization Via Response Surface Methodology, *Fuel*, **306**: 121635 (2021).
- [14] Ashenaean S, Haghghi M, Rahemi N., Hybrid Plasma-Sono-Coprecipitation Dispersion of NiMo Nanocatalyst over Functionalized Multiwall Carbon Nanotube Used in Hydrodesulfurization of Thiophene, *Adv. Powder. Technol.*, **30**: 502–512 (2019).
- [15] AL-Hammadi S.A., Al-Amer A.M., Saleh T.A., Alumina-Carbon Nanofiber Composite as a Support for MoCo Catalysts in Hydrodesulfurization Reactions, *Chem. Eng. J.*, **345**: 242–251 (2018).

- [16] Han W., Nie H., Long X., Li M., Yang Q., Li D., Effects of the Support Brønsted Acidity on the Hydrodesulfurization and Hydrodenitrogenation Activity of Sulfided NiMo/Al<sub>2</sub>O<sub>3</sub> Catalysts, *Catal. Today*, **292**: 58–66 (2017).
- [17] Kaluža L., Zdražil M., Carbon-Supported Mo Catalysts Prepared by a New Impregnation Method Using a MoO<sub>3</sub>/Water Slurry: Saturated Loading, Hydrodesulfurization Activity and Promotion by Co, *Carbon N Y*, **39**:2023–2034 (2001).
- [18] Kohli K., Prajapati R., Maity S.K., Sharma B.K., Effect of Silica, Activated Carbon, and Alumina Supports on NiMo Catalysts for Residue Upgrading, *Energies*, **13**: 1–16 (2020).
- [19] Argyle M.D., Bartholomew C.H., Heterogeneous Catalyst Deactivation and Regeneration: A Review, *Catalysts*, **5**: 145–269 (2015).
- [20] Liu M., Zhang L.Z., Zhang C., Yuan S.H., Zhao D.Z., Duan L.H., Transformation of Nitrogen-Containing Compounds in Atmospheric Residue by Hydrotreating, *Korean. J. Chem. Eng.*, **35**: 375–382 (2018).
- [21] Liakakou E.T., Heracleous E., Triantafyllidis K.S., Lemonidou A.A., K-Promoted NiMo Catalysts Supported on Activated Carbon for the Hydrogenation Reaction of CO to Higher Alcohols: Effect of Support and Active Metal, *Appl. Catal. B Environ.*, **165**: 296–305 (2015).
- [22] Gu L., Dong G., Yu H., Zhang K., Lu X., Wen H., et al., Preparation of Porous Biochar by Urine Assisted Pyrolysis of Sewage Sludge and their Application for Eriochrome Black T Adsorption, *J. Anal. Appl. Pyrolysis*, **153**:104975 (2020).
- [23] Sekirifa M.L., Hadj-Mahammed M., Pallier S., Baameur L., Richard D., Al-Dujaili A.H., Preparation and Characterization of an Activated Carbon from a Date Stones Variety by Physical Activation with Carbon Dioxide, *J. Anal. Appl. Pyrolysis*, **99**: 155–160 (2013).
- [24] Ahmadpour A, Do DD., The Preparation of Active Carbons from Coal by Chemical and Physical Activation, *Carbon N Y*, **34**: 471–479 (1996).
- [25] Maciá-Agulló J.A., Moore B.C., Cazorla-Amorós D., Linares-Solano A., Activation of Coal Tar Pitch Carbon Fibres: Physical Activation vs. Chemical Activation, *Carbon N Y*, **42**: 1367–1370 (2004).
- [26] Hosseini M., Hatefirad P., Salimi S., Tavasoli A., Hydrothermal Liquefaction of Granular Bacteria to High-Quality Bio-Oil Using Ni–Ce Catalysts Supported on Functionalized Activated Carbon, *Energy*, **241**: 122875 (2021).
- [27] Nath Prajapati Y., Verma N., Hydrodesulfurization of Thiophene on Activated Carbon Fiber Supported NiMo Catalysts, *Energy and Fuels*, **32**: 2183–2196 (2018).
- [28] Akcil A., Vegliò F., Ferella F., Demet M., Tuncuk A., A Review of Metal Recovery from Spent Petroleum Catalysts and Ash, *Waste Manag*, **45**: 420–433 (2015).
- [29] Abbas M.N., Alalwan H.A., Catalytic Oxidative and Adsorptive Desulfurization of Heavy Naphtha Fraction, *Korean Chemical Engineering Research*, **57**: 1–6 (2019).
- [30] Sakanishi K., Nagamatsu T., Mochida I., Whitehurst D.D., Hydrodesulfurization Kinetics and Mechanism of 4,6-dimethyldibenzothiophene over NiMo Catalyst Supported on Carbon, *J. Mol. Catal. A Chem.*, **155**: 101–109 (2000).
- [31] Kim J.H., Ma X., Song C., Lee Y., Oyama S.T., Kinetics of Two Pathways for 4,6-dimethyldibenzothiophene Hydrodesulfurization over NiMo, CoMo Sulfide, and Nickel Phosphide Catalysts, *Energy Fuels*, **19**: 353–364 (2005).
- [32] Lam E., Luong J.H.T., Carbon Materials as Catalyst Supports and Catalysts in the Transformation of Biomass to Fuels and Chemicals, *ACS Catal*, **4**: 3393–3410 (2014).
- [33] Liu L., Ji M., Wang F., Adsorption of Nitrate onto ZnCl<sub>2</sub>-Modified Coconut Granular Activated Carbon: Kinetics, Characteristics, and Adsorption Dynamics, *Adv. Mater. Sci. Eng.*, (2018).
- [34] Zhu Q.L., Xu Q., Immobilization of Ultrafine Metal Nanoparticles to High-Surface-Area Materials and their Catalytic Applications, *Chem.*, **1**: 220–245 (2016).
- [35] Zhang J., Li X., Chen H., Qi M., Zhang G., Hu H., et al., Hydrogen Production by Catalytic Methane Decomposition: Carbon Materials as Catalysts or Catalyst Supports, *Int. J. Hydrogen Energy*, **42**: 19755–19775 (2017).
- [36] Hatefirad P, Tavasoli A., Effect of Acid Treatment and Na<sub>2</sub>CO<sub>3</sub> as a Catalyst on the Quality and Quantity of Bio-Products Derived from the Pyrolysis of Granular Bacteria Biomass, *Fuel*, **295**: 120585 (2021).

- [37] Karimnezhad L., Haghghi M., Fatehifar E., Adsorption of Benzene and Toluene from Waste Gas Using Activated Carbon Activated by ZnCl<sub>2</sub>, *Front Environ Sci Eng*, **8**: 835–844 (2014).
- [38] Rasool T., Srivastava V.C., Khan M.N.S., Utilisation of a Waste Biomass, Walnut Shells, to Produce Bio-Products via Pyrolysis: Investigation Using ISO-Conversional and Neural Network Methods, *Biomass Convers Biorefinery*, **8**: 647–657 (2018).
- [39] Açıklan K., Thermogravimetric Analysis of Walnut Shell as Pyrolysis Feedstock, *J. Therm. Anal. Calorim.*, **105**: 145–150 (2011).
- [40] Uzun B.B., Yaman E., Pyrolysis Kinetics of Walnut Shell and Waste Polyolefins Using Thermogravimetric Analysis, *J Energy Inst*, **90**: 825–837 (2017).
- [41] Xu J., Cao X., Characterization and Mechanism of MoS<sub>2</sub>/CdS Composite Photocatalyst Used for Hydrogen Production from Water Splitting Under Visible Light, *Chem. Eng. J.*, **260**: 642–648 (2015).
- [42] Abubakar U.C., Alhooshani K.R., Adamu S., Al Thagfi J., Saleh T.A., The Effect of Calcination Temperature on the Activity of Hydrodesulfurization Catalysts Supported on Mesoporous Activated Carbon, *J. Clean. Prod.*, **211**: 1567–1575 (2019).
- [43] Saleh T.A., The Influence of Treatment Temperature on the Acidity of MWCNT Oxidized by HNO<sub>3</sub> or a Mixture of HNO<sub>3</sub>/H<sub>2</sub>SO<sub>4</sub>, *Appl. Surf. Sci.*, **257**: 7746–7751 (2011).
- [44] Saleh T.A., Simultaneous Adsorptive Desulfurization of Diesel Fuel over Bimetallic Nanoparticles Loaded on Activated Carbon, *J. Clean. Prod.*, **172**: 2123–2132 (2018).
- [45] Rambabu N., Badoga S., Soni K.K., Dalai A.K., Adjaye J., Hydrotreating of Light Gas Oil Using a NiMo Catalyst Supported on Activated Carbon Produced from Fluid Petroleum Coke, *Front. Chem. Sci. Eng.*, **8**: 161–170 (2014).
- [46] Abubakar U.C., Alhooshani K.R., Adamu S., Al Thagfi J., Saleh T.A., The Effect of Calcination Temperature on the Activity of Hydrodesulfurization Catalysts Supported on Mesoporous Activated Carbon, *J. Clean. Prod.*, **211**: 1567–1575 (2019).
- [47] Ding L., Zheng Y., Zhang Z., Ring Z., Chen J., Hydrotreating of Light Cycled Oil Using WNi/Al<sub>2</sub>O<sub>3</sub> Catalysts Containing Zeolite Beta and/or Chemically Treated Zeolite Y., *J. Catal.*, **241**: 435–445 (2006).
- [48] Mahmoudabadi Z.S., Rashidi A., Tavasoli A., Synthesis of MoS<sub>2</sub> Quantum Dots as a Nanocatalyst for Hydrodesulfurization of Naphtha: Experimental and DFT Study, *J. Environ. Chem. Eng.*, **8** (2020).
- [49] Mahmoudabadi Z.S., Tavasoli A., Rashidi A., Esrafil M., Catalytic Activity of Synthesized 2D MoS<sub>2</sub>/Graphene Nanohybrids for the Hydrodesulfurization of SRLGO: Experimental and DFT Study, *Environ. Sci. Pollut. Res.*, **28**: 5978–5990 (2021).
- [50] Hita I., Palos R., Arandes J.M., Hill J.M., Castaño P., Petcoke-Derived Functionalized Activated Carbon as Support in a Bifunctional Catalyst for Tire Oil Hydroprocessing, *Fuel Process Technol.*, **144**: 239–247 (2016).
- [51] Román-Martínez M.C., Cazorla-Amorós D., Linares-Solano A., de Lecea C.S.M., TPD and TPR Characterization of Carbonaceous Supports and Pt/C Catalysts, *Carbon N Y*, **31**: 895–902 (1993).
- [52] Nabgan W., Rashidzadeh M., Nabgan B., The Catalytic Naphtha Reforming Process: Hydrodesulfurization, Catalysts and Zeofoming, *Environ. Chem. Lett.*, **16**: 507–522 (2018).
- [53] Farag H., Hydrodesulfurization of Dibenzothiophene and 4,6-dimethyldibenzothiophene over NiMo and CoMo sulfide Catalysts: Kinetic Modeling Approach for Estimating Selectivity, *J. Colloid. Interface. Sci.*, **348**: 219–226 (2010).
- [54] Abid M.F., Ahmed S.M., Abohameed W.H., Ali S.M., Study on Hydrodesulfurization of a Mixture of Middle Distillates, *Arab. J. Sci. Eng.*, **43**: 5837–5850 (2018).
- [55] Behnejad B., Abdouss M., Tavasoli A., Ni-mo Supported Nanoporous Graphene as a Novel Catalyst for HDS and Hdn of Heavy Naphtha, *Brazilian J. Chem. Eng.*, **36**: 265–273 (2019).
- [56] Behnejad B., Abdouss M., Tavasoli A., Comparison of Performance of Ni–Mo/γ-alumina Catalyst in HDS and HDN Reactions of Main Distillate Fractions, *Pet. Sci*, **16**: 645–656 (2019).
- [57] Behnejad B., Abdouss M., Tavasoli A., Effect of Graphene Functionalizing on the Performance of NiMo/Graphene in HDS and HDN Reactions, *Pet. Sci.*, **16**: 1185–1195 (2019).